Journal of Computers and Applied Science Education Volume 2, Number 2, 2015

Theoretical investigation of ferromagnetism of graphene induced from gas adsorptions

Chih-Min Ku and Shih-Jye Sun*
Department of Applied Physics, National University of Kaohsiung, Kaohsiung 811,Taiwan
sjs@nuk.edu.tw

ABSTRACT. *Ferromagnetism of hydrogenated graphene is very signi_cant to graphene which adsorbs hydrogen gases so as to become ferromagnetic. Inspired by the fact, we setup a theoretical Hamiltonian model in this study, instead of the _rst principle calculations. To investigate what conditions the ferromagnetism of graphene would appear in, we utilize a set of energy parameters which are correspondent to the adsorbed gas. Actually, we found the reduced hopping integral along the gas adsorption sites and the Coulomb repulsions on gas adsorption sites as well as nearby sites are both important factors for the ferromagnetism appearance. Speci_cally, we propose the Rashba spin-orbit interaction arising from the structure symmetry broken it should appear by means of distorting the structure via the gas adsorption. Through the triumphing results of calculations in this study, we found that as the ferromagnetism of graphene induced from gas adsorption, the Rashba spin-orbit interaction could have the possibility to enhance the ferromagnetism.*

PACS numbers: 75.50.-y,81.05.ue,75.10.Jm

1. Introduction

As being ideally flat, graphene possesses extremely high mobility, which arises from a nearly gapless band structure and facilitates the graphene to have an outstanding potential to be some conductor applications [1, 2].The graphene would possess the electrical function via traditional electrons to open a proper gap on itself [3]. However, this theory consists toughly manipulating process and causes the reduced mobility as well [4, 5]. Thus there is a tradeoff between the band gap opening and the proper electric mobility to yield graphenebased semiconductor devices. Since single functional channel devices, e.g., either electrical or magnetic devices, do not satisfy our demand in this modern technological era anymore, thus the multifunctional channel devices, i.e., manipulate a device called spintronics by charge and spin simultaneously, are hot to be pursued [6, 7]. Of course, spintronics will become crucial devices of next generation [8]. In other words, the spintronics materials are much better at becoming ferromagnetic, otherwise there are no spins to be manipulated [9, 10]. Unfortunately, a pure graphene is essentially nonmagnetic, except we make some efforts to modify the graphene in the ferromagnetic extent [11-14]. Up to now, many methods have been employed to make the ferromagnetism appear on the graphene, for instance, to dope ions or to make defects on graphene

[15-18], or to hydrogenate graphene [19-24], etc. Obviously, the last method seems simple and easy to proceed.

Actually, graphene has been proven to have the gas adsorption capability with the responses to some property variations [25-27]. For instance, the electrical conductivity of graphene will be varied in gas adsorptions, thus which promote the graphene to be a candidate as a gas sensor material [28, 29]. As our realization, the graphene begins adsorbing gases just by means of dangling bonds, which arise from one of three p orbits of each carbon atom exposing to outside plane of the graphene sheet [30]. In particular, a ferromagnetic graphene has been predicted from the first principle calculations as it adsorbs hydrogen gases [31, 32], i.e., hydrogenating graphene. This prediction also has been confirmed from recent experiments [21, 22]. The intriguing result also stimulates and challenges us to investigate its ferromagnetic mechanism from the gas adsorption because carbon and hydrogen elements both are light atoms without any magnetic orbits, e.g. d or f orbits, inside. Besides, the first principle calculations also have predicted that the graphene will be distorted locally from the flat structure to the three dimensional one due to the atomic bonds switching from sp^2 to quasi-sp^3 [31, 33, 34]. By virtue of the structural distortion, an interaction called Rashba spin-orbit interaction will be induced by the structure symmetry broken [35-37]. Furthermore, the experiments and theories reveal that the induced spin-orbit interaction will be enhanced to a significant level and produces an operational channel for us to manipulate the graphenebased devices[38, 39]. Since the ferromagnetism could be induced from the hydrogen gas adsorption, the possible properties induced from the other gases are expected [40].

From the above prediction, we propose two assumptions in terms of (a) the ferromagnetism induced in graphene by means of the gas adsorption arises from the Coulomb excitation, namely, so-called Stoner excitations, (b) the Coulomb repulsions appearing on the gas adsorption sites and nearby sites are induced from the carrier localization and bond distortion, respectively. Based on the two proposals, we calculate the ferromagnetism appearing on gas adsorption sites and nearby sites, and then investigate the conditions which ferromagnetism will be induced in, such as the magnitudes between Coulomb and spinorbit interactions, as well as the modified carbon orbital energy and hopping integral, the ferromagnetism will be induced.

In this study, we accomplished the magnetic phase diagrams in accordance with functions of modified carbon orbital energies with various Coulomb repulsions for the ferromagnetism, which appears on gas adsorption sites and nearby sites. The studied result indicates that the ferromagnetism preferential appears on gas adsorption sites, as the Coulomb repulsion on gas adsorption sites is larger than that on nearby sites. On contrary, another phenomenon occurs in response to opposite conditions, i.e., the Coulomb repulsion on gas adsorption sites is less than that on nearby sites. In particular, from the calculation results of the study, we found a key factor for the ferromagnetism formation is the hopping integral, which could be modified and reduced from the gas adsorption. To be specific, the ferromagnetism only survives on a variously reduced hopping integral along the gas adsorbed bonds.

The most triumphing result from our investigations reveals that the ferromagnetism on gas adsorption sites could be enhanced with the increase of Rashba spin-orbit interaction in some energy parameters conditions.

The structure of the paper is organized as the following structures. The section II demonstrates the theoretical descriptions. The section III shows the studied results to be accompanied by the discussions as well. Eventually, in the last section we sort all conclusions from investigations in the study.

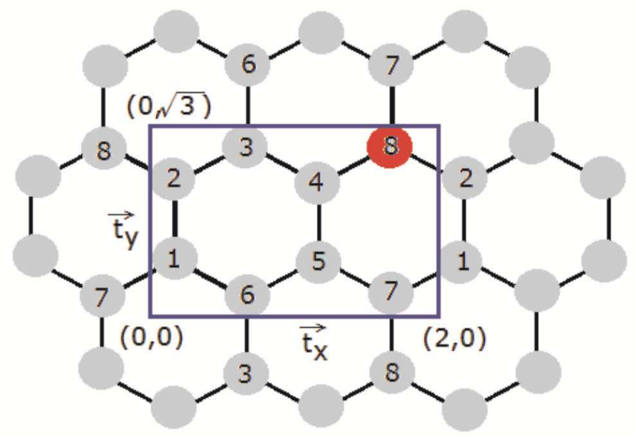

FIG. 1: The unit cell of gas adsorbed graphene is depicted in a blue rectangular with unit vectors, $\vec{t}_x = (2,0)$ and $\vec{t}_y = (0,\sqrt{3})$. The unit cell includes 8 carbon atoms indexed the integral integrals from 1~ 8 and the gas is adsorbed on the 8th carbon atom marked with red color.

2. Theory

For simplicity in the theoretical investigation, we set up a rectangular unit cell of a graphene and the unit vectors in the unit cell are $\vec{t}_x = (2,0)$ and $\vec{t}_y = (0,\sqrt{3})$, respectively. The unit cell includes 8 carbon atoms and one of them adsorbs a gas molecule, as depicted in Fig. 1. The gas adsorption site in the unit cell is indexed by 8 and the nearby sites are indexed by 2, 4 and 7 as well. In this simple gas adsorption structure, the gas adsorption rate is 1/8. and we also exclude two adsorbed gases are neighboring and at least it is rational at dense adsorption cases [41]. This exclusion is based on the Coulomb repulsion between two gas molecules repelling to each other. Even though the specific gas adsorption rate was proposed for the investigation, we suppose the ferromagnetic properties induced from the gas adsorption in different adsorption rates are qualitatively similar.

The Hamiltonian of the gas adsorbing system includes three sub-Hamiltonian,

$$H = H_0 + H_U + H_{SOC} \tag{1}$$

These sub-Hamiltonian are the kinetic energy, H_0, Coulomb interaction, H_U, orbital energy, and Rashba spin-orbit interaction, H_{SOC}, and their mathematic representations can be written respectively as,

$$H_0 = \sum_{<<i,j>>,\sigma} t_{i,j} c_{i,\sigma} + c_{j,\sigma} \tag{2}$$

where *i* and *j* are the site indexed from 1 to 8, σ is the spin index and $t_{i,j}$ is the hopping integral between sites *i* and *j*. The operators c^+ and *c* are creation and annihilation operators for the carriers in carbon atoms. Since we employ the tight-binding model to this work, the double bracket << *i, j* >> means that only the nearest-neighbor interactions are considered and the hopping integral t is taken as a constant. In addition, due to the bond distortion around the adsorbed gases, the hopping integral will be reduced along the gas adsorbed bonds.

$$H_U = \sum_i U_i n_{i,\uparrow} n_{i,\downarrow}. \tag{3}$$

This term represents the Coulomb repulsions on the carbon sites, as both up and down spin carriers simultaneously appear on a site. U_i is the Coulomb repulsion on the *i*th site and $n_{i,\uparrow}(n_{i,\downarrow})$ represents the up spin (down spin) carrier density. In our calculations, we only suppose the Coulomb repulsions appear on the gas adsorption sites and nearby sites. Both the former and the latter arise from the carrier localization and the bond distortion, respectively.

$$H_{SOC} = iV_{Rb} \sum_{<i,j>} \mu_{i,j} c_{i,\alpha} + (\vec{\sigma} \times \hat{d}_{i,j})^z_{\alpha\beta} c_{j,\beta} \tag{4}$$

This term is called Rashba spin-orbit interaction induced from the structure symmetry broken. This interaction just appears along A to A or B to B sites in the sub-lattice graphene [42]. V_{Rb} is the spin-orbit interaction strength. The vector $\hat{d}_{ij} = (\hat{d}^x_{ij}, \hat{d}^y_{ij})$ means the unit vector from site *i* to site *j* in the sub-lattice A or B and $\mu_{i,j} = 1(-1)$ for A sub-lattice (B sub-lattice). α and β are spin indexes for the spin with one half. After simple algebraic derivations, the term $(\vec{\sigma}\times\hat{d}_{ij})^{z}_{\alpha\beta}$ results in a simple matrix form as a function of α, while $\alpha = \hat{d}^{x}_{ij} + \mathrm{i}\ \hat{d}^{y}_{ij}$.

$$(\vec{\sigma}\times\hat{d}_{i,j})^{z}_{\alpha\beta} = \begin{pmatrix} 0 & \alpha \\ \alpha^{*} & 0 \end{pmatrix} \tag{5}$$

For further simplifying our problem, we take the Hatree mean field approximation to H_U and results in,

$$\bar{H}_U = \sum_{i\in\{2,4,7,8\}} \{U_i \left(\left\langle n_{i,\downarrow}\right\rangle n_{i,\uparrow} + \left\langle n_{i,\uparrow}\right\rangle n_{i,\downarrow}\right) - U_i \left\langle n_{i,\uparrow}\right\rangle \left\langle n_{i,\downarrow}\right\rangle\}. \tag{6}$$

Furthermore, based on the tight-binding model, the momentum presentation of the Hamiltonian element $H(\vec{k})_{i,j} = H_{i,j}\sum_{\vec{R}\in\{\vec{t}_x,\vec{t}_y\}} \exp(i\vec{k}\cdot(\vec{R}+(\vec{d}_j-\vec{d}_i)))$, where $\vec{d}_i$ means the coordinate of the *i*th site and $\vec{R}$ is $\pm\vec{t}_x$, $\pm\vec{t}_y$ or $\pm\vec{t}_x\pm\vec{t}_y$ for different sites to satisfy the periodic boundary conditions. Moreover, we suppose the charge transfer should not take place during the gas adsorption process, namely, each carbon site keeps the carrier number constant as well as unit. Based on above approximations, the free energy of the system can be written as,

$$\begin{aligned} F_{MF} &= -\frac{1}{\beta}\sum_{\sigma,i,k} \ln\{1+\exp[\beta(\mu - E_i(k))]\} \\ &\quad - \sum_{i\in\{2,4,7,8\}} U_i \left\langle n_{i,\uparrow}\right\rangle \left\langle n_{i,\downarrow}\right\rangle. \end{aligned} \tag{7}$$

$\beta = \frac{1}{k_B T}$ is the inverse temperature energy, μ is the chemical potential obtained from carriers conservation and $E_i(k)$ is the *i*th eigenvalue of $H(k)$. Since the up spin and down spin carrier number, $\left\langle n_{i,\uparrow}\right\rangle$ and $\left\langle n_{i,\downarrow}\right\rangle$ on each carbon site, can be obtained by minimizing the free energy F_{MF} . Consequently the net magnetic moment on each site is eventually obtained by,

$$m_i = \frac{1}{2}\left(\left\langle n_{i,\uparrow}\right\rangle - \left\langle n_{i,\downarrow}\right\rangle\right). \tag{8}$$

Since sites 2, 4 and 7 are symmetrically located around the site 8, the magnetic moments on these sites should be equal to one another thus we average their magnetic moments to gain the individual value of each site. On account of the asymmetric unit cell, the different magnetic moments are obtained from the calculations. Based on our theoretical Hamiltonian model, some energy parameters are closely related to the formation of the ferromagnetism, which are Coulomb repulsions, E_H, U_n and orbital energies, E_{CH}, E_{CN}, on adsorption sites and nearby carbon sites, respectively, as well as the modified hopping integral t_H due to the gas adsorption. The U_H arises from the gas adsorption, which causes the original π orbits of carbon to be rather localized and to increase the Coulomb repulsions. As the grapheme adsorbs the gases, the original sp2 orbital bonds will be transformed to sp3, which result in a structure distortion from a flat form to a three dimensional one and accompany the orbital bonds connected with gas adsorption nearby sites to be tilled. Consequently, U_n will be formed. Similarly, due to the gas adsorption, the original orbital energy, E_C, on each carbon site, will be transformed into E_{CH} or E_{CN} respectively, such two types of which depend on the verified orbital energies of being on gas adsorption sites or nearby sites. From our calculations, the conditions for ferromagnetism appearing on gas adsorption sites and nearby sites are very different. In particular, the modified hopping integral t_H is a very dominant parameter for forming the ferromagnetism. We found the t_H should be reduced very seriously, otherwise no ferromagnetism will appear. Actually, the t_H will be reduced as graphene adsorbs gases. The phenomenon seems reasonable since the carriers hopping easily in original sp2 bonds will be reduced in tilled sp3 bonds. Basically, we propose a set of U_H, U_n, t_H, E_{CH} and E_{CN} to simulate an individual adsorbed gas and all of the energies are scaled by the original hopping integral *t*.

3. Results and discussions

Firstly, we construct the phase diagrams of the ferromagnetism for the gas adsorption sites and nearby sites in order to investigate what conditions the ferromagnetism of grapheme will appear in. Fig. 2(a) is the phase diagram of the ferromagnetism appearing on the gas adsorption sites with different E_{CH} and E_{CN}. Herein, the Coulomb repulsions are set to $U_H / t = 2$ and $U_n / t = 1$, respectively, where U_H is larger than U_n. Obviously, the ferromagnetism mostly appear on graphene as E_{CH} and E_{CN} both are negative and positive, respectively, except a small portion of ferromagnetic phase appearing on both orbital energies with negative E_{CH} and E_{CN} simultaneously. In spite of the exceptional small portion, the E_{CH} is still lower than E_{CN}. Namely, the dominant appearance of ferromagnetism on gas adsorption sites is determined on the orbital energy of gas adsorption sites lower than that of nearby sites. In the model, we set U_H larger than U_n is assumed that U_n induced from the bond distortion is serious no more than U_H induced from the carrier localization. Similarly, the phase diagram of the ferromagnetism appearing on gas adsorption nearby sites with different E_{CH} and E_{CN} is shown in Fig. 2(b). In the same Coulomb repulsion conditions, we can find that the ferromagnetism in the same ferromagnetic phase part for nearby sites is negative, namely, antiferromagnetic to the gas adsorption sites. Besides, in the phase diagram, only very small part shows ferromagnetism with simultaneously positive E_{CH} and E_{CN} appears on gas adsorption sites and nearby sites. The particular part is only likely to exist on the boundaries of the above mentioned main regions, where ferromagnetism on gas adsorption sites and nearby sites is antiferromagnetically aligned.

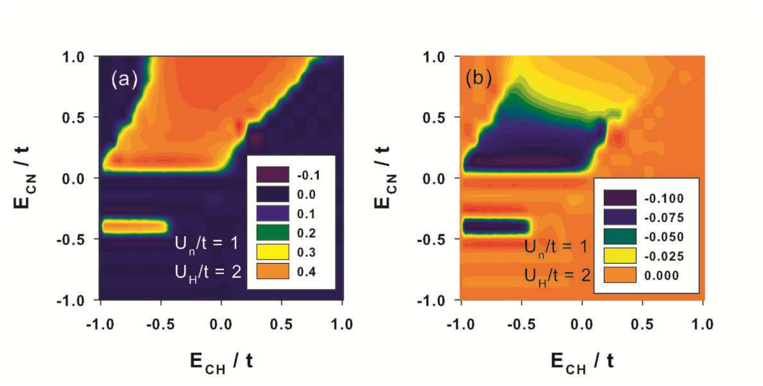

FIG. 2: The phase diagram of the ferromagnetism appears on (a) the gas adsorption sites. (b) the gas adsorption nearby sites. The Rashba V_{Rb} and the reduced hopping integral t_H are set to 0.1 t and 0.25 t, respectively.

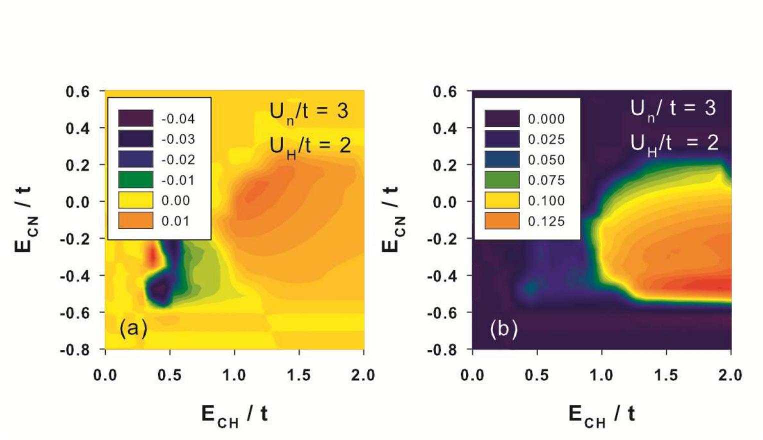

FIG. 3: The phase diagram of the ferromagnetism appearing on (a) the gas adsorption sites. (b) the gas adsorption nearby sites. The Rashba V_{Rb} and the reduced hopping integral t_H are set to 0.1 t and 0.25 t respectively.

In spite of U_n increasing with much serious bond distortion, it could be even larger than the U_H induced from the orbital localization by gas adsorption. Fig. 3(a) represents the ferromagnetic phase diagram for the ferromagnetism on gas adsorption sites with different E_{CH} and E_{CN} as $U_n / t = 3$ and $U_n / t = 2$. Two dominant and small regions with positive ferromagnetism appear on either positive high E_{CH} and positive low E_{CN}, or positive low E_{CH} and negative low E_{CN}, respectively. Obviously, the ferromagnetism appearing on gas adsorption sites are suppressed, as U_H is lower than U_n. On the contrary, the ferromagnetism preferential appears on the gas adsorption nearby sites as shown in Fig. 3(b), which reveals a larger region with ferromagnetism. The results also imply that a seriously distorted grapheme is induced from the gas adsorption and the ferromagnetism seems preferentially appearing on gas adsorption nearby sties.

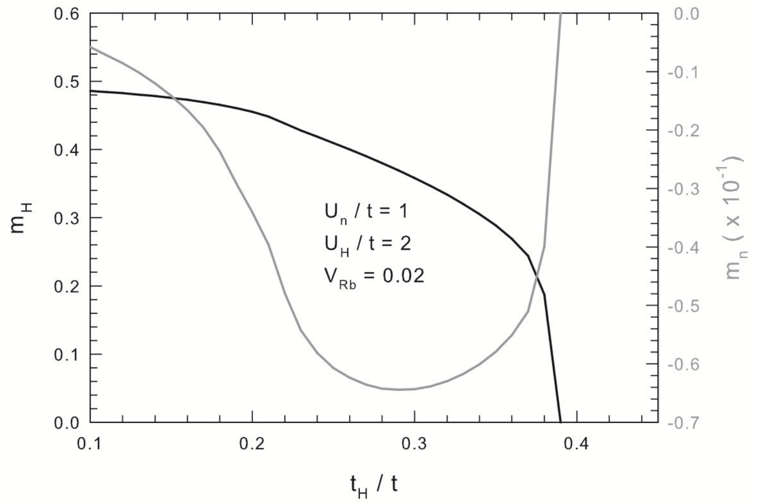

FIG. 4: The ferromagnetism on gas adsorption sites (black curves) and nearby sites (dark gray curve) as a function of reduced hopping integral, t_H. The orbital energies for gas adsorption sites and nearby sites, E_{CH} and E_{CN}, are set to -0.5 t and 0.5 t, respectively.

As aforementioned, the hopping integral, t_H, varied with gas adsorption, is a very important factor for the ferromagnetism formation. We found that the ferromagnetism appearing on either the gas adsorption sites or nearby sites needs a reduced t_H in comparison with original hopping integral *t*. Fig. 4 clearly shows that the ferromagnetism will disappear as t_H is too large. Herein, we just show $U_H > U_n$ case and add a small Rashba spin-orbit interaction to simulate the spin-orbit interaction induced from the structure distortion. Actually, for $U_n > U_H$ case, the result is similar. Furthermore, the ferromagnetism on gas adsorption sites reaches a maximum as t_H is zero. The phenomenon also implies that ferromagnetism preferential appears on an insulating graphene. On the contrary, the maximum ferromagnetism appears antiferromagnetic on gas adsorption nearby sites in a finitely reduced t_H, which rationally means that the ferromagnetism induced on these nearby sites still needs mobile carriers hopping to these sites.

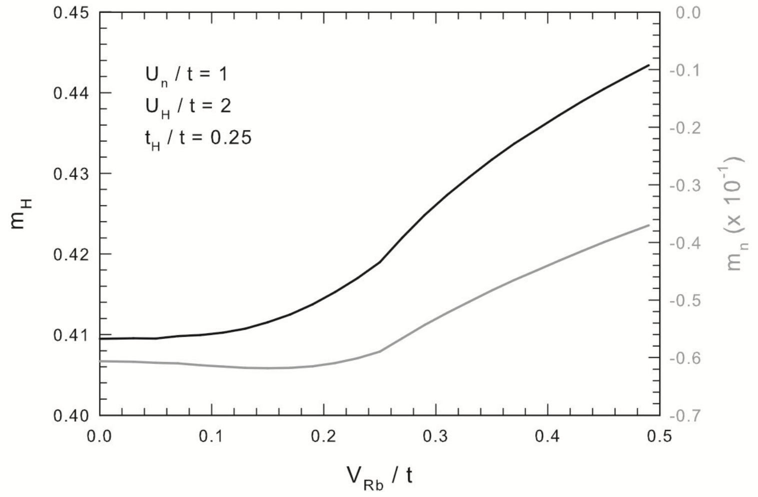

FIG. 5: The ferromagnetism on gas adsorption sites (black curves) and nearby sites (dark gray curve) as a function of Rashba spin-orbit interaction. The orbital energies, E_{CH} and E_{CN} are set to -0.5 t and 0.5 t, respectively.

As our realization, the intrinsic spin-orbit interaction is so weak as to be ignored, even though the graphene adsorbs some heavy gases. However, if the graphene structure is distorted after the gas adsorption, the Rashba spin-orbit interaction, V_{Rb}, induced from the structure symmetry broken will be significant. Interestingly, we found the ferromagnetism on gas adsorption sites could increase with V_{Rb}; while the ferromagnetism on gas adsorption nearby sites could be suppressed as shown in Fig. 5. We suppose the increase on gas adsorption sites result from the spins on nearby sites hopping as well as flipping to gas adsorption sites by means of the Rashba interaction. Basically, the spin flipping process could be easily recognized from the eq. 5, which is the intrinsic characteristic of Rashba interaction different from the intrinsic spin-orbit interaction where the spins do not flip. Furthermore, the above result implies the hydrogen gas is the best medium to induce the ferromagnetism because carbon-hydrogen bonds will be transferred to highly distorted sp3 bonds, which increases the Rashba interaction as well as reduces the hopping integral. Actually, Fig. 5 only exhibits a qualitative property, because the magnitude of the V_{Rb} processing large enough influence on ferromagnetism is overestimated in comparison with the prediction from the experiments. We assume that the overestimation arises from the mean field theory which is based on a simple and accessible model. Actually, t_H and V_{Rb} both interactions are in a simultaneous response, namely, a further seriously distorted structure will cause a rather reduced t_H and increased V_{Rb}, respectively.

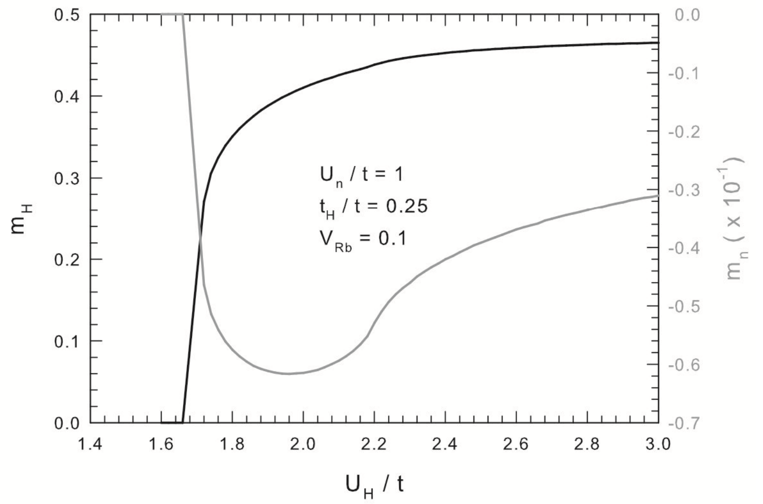

FIG. 6: The ferromagnetism on gas adsorption sites (black curves) and nearby sites (dark gray curve) as a function of Coulomb repulsion, U_H, on adsorption sites. The orbital energies, E_{CH} and E_{CN}, are set to -0.5 t and 0.5 t, respectively.

As our model proposed, the ferromagnetism induced from the gas adsorption possibly appears on either the adsorption sites or nearby sites by means of Coulomb excitations. Fig. 6 shows the ferromagnetism m_H and m_n on adsorption sites and nearby sites, respectively, as a function of Coulomb repulsion, U_H, on adsorption sites. The results were calculated via the properly estimated parameters with the Coulomb repulsions, $U_n / t = 1$on nearby sites, and the hopping integrals, $t_H / t = 0.25$, reduced from the bond distortion by gas adsorption. Specially, the gas adsorption not only makes the structure distortion, but also causes the structure symmetry broken, which induces the Rashba spin-orbit interaction, V_{Rb} as well. According to the experimental reports, the V_{Rb} is significant, thus in the model, we put a considerable $V_{Rb} = 0.1$in the calculation in order to observe the interaction effect on the ferromagnetism. In Fig. 6 the magnitude of ferromagnetism on the gas adsorption sites is larger than on nearby sites. The m_H increases rapidly with the U_H and a critical U_H^* exists to appear ferromagnetism as U_H is larger than that. Besides, in the most portion of U_H, the m_n shows negative, which means the m_H and m_n are antiferromagnetic. Furthermore, an optimal magnetization m_n appears around $U_H / t = 2$. All data in Fig. 6 represent the findings that m_H and m_n are closely related to each other and are active in the competition as well.

4. Conclusion

In this study, we accomplished the magnetic phase diagrams, as the ferromagnetism appears on gas adsorption sites and nearby sites in correspondence with functions of modified carbon orbital energies as well as various Coulomb repulsions. As the Coulomb repulsion on gas adsorption sites, U_H, is larger than that on nearby sites, U_n, the variation of whether the ferromagnetism preferential appears on gas adsorption sites is determined on the orbital energy of gas adsorption sites, E_{CH}, lower than that of nearby sites, E_{CN}. On the contrary, under the same Coulomb repulsion conditions for the same ferromagnetic phase regions, the ferromagnetism on nearby sites are negative, namely, antiferromagnetic to gas adsorption sites. As the Coulomb repulsion on gas adsorption sites is less than that on nearby sites, both dominant and minor regions appear positive ferromagnetism with either high positive E_{CH} and low positive E_{CN}, or low positive E_{CH} and low negative E_{CN}, respectively. Obviously, the ferromagnetism appearing on gas adsorption sites are suppressed as U_H is lower than U_n namely, the ferromagnetism preferential appears on the gas adsorption nearby sites. The most key factor for the ferromagnetism induction from the gas adsorption is the hopping integral which is modified and reduced from the bond distortion. Furthermore, the Rashba spin-orbit interaction will be induced from the structure symmetry broken by gas adsorption. Specifically, we found that the ferromagnetism on gas adsorption sites has the possibility to increase with the Rashba spin-orbit interaction, by contrast, the ferromagnetism on gas adsorption nearby sites will be suppressed.

Acknowledgement

We would like to thank the support by the Ministry of Science and Technology of Republic of China for Grant No. NSC-101-2112-M-390-001-MY3. The hospitality of the National Center for Theoretical Sciences, Taiwan, where the work was initiated, is gratefully acknowledged.

References

K. S. Novoselov, A. K. Geim, S. V. Morozov, D. Jiang, M. I. Katsnelson, I. V. Grigorieva, S. V. Dubonos, and A. A. Firsov (2005). *Two-dimensional gas of massless Dirac fermions in graphene*, Nature 438, 197.

A. H. Castro Neto, F. Guinea, N. M. R. Peres, K. S. Novoselov, and A. K. Geim (2009). *The electronic properties of graphene*, Rev. Mod. Phys. 81, 109.

Richard Balog, Bjarke Jørgensen, Louis Nilsson, Mie Andersen, Emile Rienks, Marco Bianchi, Mattia Fanetti, Erik Lægsgaard, Alessandro Baraldi, Silvano Lizzit, Zeljko Sljivancanin, Flemming Besenbacher, Bjørk Hammer, Thomas G. Pedersen, Philip Hofmann, and Liv Hornekær (2010), *Bandgap opening in graphene induced by patterned hydrogen adsorption*, Nature Materials 9, 315.

Tomás Palacios (2011). *Graphene electronics: Thinking outside the silicon box*, Nature Nanotechnology 6, 464.

S. Y. Zhou, G.-H. Gweon, A. V. Fedorov, P. N. First, W. A. de Heer, D.-H. Lee, F. Guinea, A. H. Castro Neto, and A. Lanzara (2007). *Substrate-induced bandgap opening in epitaxial graphene*, Nature Materials 6, 770.

Igor Žutić, Jaroslav Fabian, and S. Das Sarma (2004). Spintronics: Fundamentals and applications, Rev. Mod. Phys. 76, 323.

Dmytro Pesin, Allan H. MacDonald (2012). *Spintronics and pseudospintronics in graphene and topological insulators*, Nature Materials 11, 409.

S. A. Wolf, D. D. Awschalom, R. A. Buhrman, J. M. Daughton, S. von Molnáar, M. L. Roukes, A. Y. Chtchelkanova, D. M. Treger(2001). Spintronics: A Spin-Based Electronics Vision for the Future, Science 294, 1488.

V. A. Ivanov, T. G. Aminov, V. M. Novotortsev, V. T. Kalinnikov (2004). Spintronics and spintronics materials, Russ. Chem. Bull., 53, 2357.

Evgeny Y. Tsymbal, Spintronics: Electric toggling of magnets, Nature Materials 11, 12 (2012).

Håvard Haugen, Daniel Huertas-Hernando, and Arne Brataas (2008). *Spin transport in proximity-induced ferromagnetic graphene*, Phys. Rev. B 77, 115406.

Gábor Zsolt Magda, Xiaozhan Jin, Imre Hagymási, Péter Vancsó, Zoltán Osváth, Péter Nemes-Incze, Chanyong Hwang, László P. Biró and Levente Tapasztó (2014). *Room-temperature magnetic order on zigzag edges of narrow graphene nanoribbons*, Nature 514, 608.

Zhiyong Wang, Chi Tang, Raymond Sachs, Ya_s Barlas, and Jing Shi (2015). *Proximity-Induced Ferromagnetism in Graphene Revealed by the Anomalous Hall Effect*, Phys. Rev. Lett. 114, 016603.

P. O. Lehtinen, A. S. Foster, Yuchen Ma, A. V. Krasheninnikov, and R. M. Nieminen (2004). *Irradiation-Induced Magnetism in Graphite: A Density Functional Study*, Phys. Rev. Lett. 93, 187202.

F. Donati, Q. Dubout, G. Autès, F. Patthey, F. Calleja, P. Gambardella, O. V. Yazyev, and H. Brune (2013). *Magnetic Moment and Anisotropy of Individual Co Atoms on Graphene*, Phys. Rev. Lett. 111, 236801.

E. J. G. Santos, D. Sánchez-Portal, and A. Ayuela (2010). *Magnetism of substitutional Co impurities in graphene: Realization of single π vacancies*, Phys. Rev. B 81, 125433.

Oleg V. Yazyev and Lothar Helm, Defect-induced magnetism in graphene, Phys. Rev. B 75, 125408 (2007).

Ji-Chang Ren, Zejun Ding, Rui-Qin Zhang, and Michel A. Van Hove (2015). *Self-doping and magnetic ordering induced by extended line defects in graphene*, Phys. Rev. B 91, 045425.

P. O. Lehtinen, A. S. Foster, A. Ayuela, A. Krasheninnikov, K. Nordlund, and R. M. Nieminen (2003), *Magnetic Properties and Diffusion of Adatoms on a Graphene Sheet*, Phys. Rev. Lett. 91, 017202.

K. Tada, J. Haruyama, H. X. Yang, M. Chshiev, T. Matsui, and H. Fukuyama (2012). *Ferromagnetism in Hydrogenated Graphene Nanopore Arrays*, Phys. Rev. Lett. 107, 217203.

Lanfei Xie, Xiao Wang, Jiong Lu, Zhenhua Ni, Zhiqiang Luo, Hongying Mao, Rui Wang, Yingying Wang, Han Huang, Dongchen Qi, Rong Liu, Ting Yu, Zexiang Shen, Tom Wu, Haiyang Peng, Barbaros Özyilmaz, Kianping Loh, Andrew T. S. Wee, Ariando, and Wei Chen(2011). *Room* *temperature ferromagnetism in partially hydrogenated epitaxial graphene*, Appl. Phys. Lett. 98, 193113.

Alex Yong Sheng Eng, Hwee Ling Poh, Filip .Šaněk, Miroslav Maryško , Stanislava Matějková, Zdeněk Sofer, and Martin Pumera(2013). *Searching for Magnetism in Hydrogenated Graphene: Using Highly Hydrogenated Graphene Prepared via Birch Reduction of Graphite Oxides*, ACS Nano, 7 5930.

Martin Pumera and Colin Hong An Wong(2013). *Graphane and hydrogenated graphene*, Chem. Soc. Rev., 42, 5987.

Shayan Hemmatiyan, Marco Polini, Artem Abanov (2014). *Allan H. MacDonald, and Jairo Sinova, Stable path to ferromagnetic hydrogenated graphene growth*, Phys. Rev. B 90, 035433.

F. Schedin, A. K. Geim, S. V. Morozov, E. W. Hill, P. Blake1, M. I. Katsnelson, and K. S. Novoselov(2007). *Detection of individual gas molecules adsorbed on graphene,* Nature Materials 6, 652.

O. Leenaerts, B. Partoens, and F. M. Peeters (2008). *Adsorption of H_2O, NH_3, CO, NO_2, and NO on graphene: A first-principles study*, Phys. Rev. B 77, 125416.

Fazel Yavari, Eduardo Castillo, Hemtej Gullapalli, Pulickel M. Ajayan and Nikhil Koratkar(2012). *High sensitivity detection of NO_2 and NH_3 in air using chemical vapor deposition grown graphene,* Appl. Phys. Lett. 100, 203120.

Hyeun Joong Yoon, Do Han Jun, Jin Ho Yang, Zhixian Zhou, Sang Sik Yang, Mark Ming-Cheng Cheng (2011). *Carbon dioxide gas sensor using a graphene sheet*, Sensors and Actuators B: Chemical 157, 310.

R. Pearce, T. Iakimov, M. Andersson, L. Hultman, A. Lloyd Spetz, R. Yakimova (2011). *Epitaxially grown graphene based gas sensors for ultra sensitive NO_2 detection*, Sensors and Actuators B: Chemical 155, 451.

M. A. Akhukov, A. Fasolino, Y. N. Gornostyrev, and M. I. Katsnelson (2012). *Dangling bonds and magnetism of grain boundaries in graphene*, Phys. Rev. B 85, 115407.

D. W. Boukhvalov, M. I. Katsnelson, and A. I. Lichtenstein (2008), *Hydrogen on graphene: Electronic structure, total energy, structural distortions and magnetism from first-principles calculations*, Phys. Rev. B 77, 035427.

J. O. Sofo, Gonzalo Usaj, P. S. Cornaglia, A. M. Suarez, A. D. Hernández-Nieves, and C. A. Balseiro (2012). *Magnetic structure of hydrogen-induced defects on graphene*, Phys. Rev. B 85, 115405.

Sunmin Ryu, Li Liu, Stephane Berciaud, Young-Jun Yu, Haitao Liu, Philip Kim, George W. Flynn, and Louis E. Brus (2010). *Atmospheric Oxygen Binding and Hole Doping in Deformed Graphene on a SiO_2 Substrate,* Nano Lett., 10, 4944.

M. Z. S. Flores, P. A. S. Autreto, S. B. Legoas and D. S. Galvao (2009). *Graphene to graphane: a theoretical study*, Nanotechnology 20 465704.

Hongki Min, J. E. Hill, N. A. Sinitsyn, B. R. Sahu, Leonard Kleinman, and A. H. MacDonald (2006).

Intrinsic and Rashba spin-orbit interactions in graphene sheets, Phys. Rev. B 74, 165310.

Mahdi Zarea and Nancy Sandler (2009). *Rashba spin-orbit interaction in graphene and zigzag nanoribbons*, Phys. Rev. B 79, 165442.

Samir Abdelouahed, A. Ernst, J. Henk, I. V. Maznichenko, and I. Mertig (2010). *Spin-split electronic states in graphene: Effects due to lattice deformation, Rashba effect, and adatoms by first principles*, Phys. Rev. B 82, 125424.

Jayakumar Balakrishnan, Gavin Kok Wai Koon, Manu Jaiswal, A. H. Castro Neto, and Barbaros Özyilmaz (2013). *Colossal enhancement of spin–orbit coupling in weakly hydrogenated graphen*e, Nature Physics 9, 284.

Martin Gmitra, Denis Kochan, and Jaroslav Fabian (2013). *Spin-Orbit Coupling in Hydrogenated Graphene*, Phys. Rev. Lett. 110, 246602.

M. Wu, En-Zuo Liu and J. Z. Jiang (2008). *Magnetic behavior of graphene absorbed with N, O, and F atoms: A first-principles study*, Appl. Phys. Lett. 93, 082504.

Richard Balog, Bjarke Jørgensen, Justin Wells, Erik Lægsgaard, Philip Hofmann, Flemming Besenbacher, and Liv Hornekær(2009). *Atomic Hydrogen Adsorbate Structures on Graphene*, J. AM. CHEM. SOC. 131, 8744.

Cheng-Cheng Liu, Hua Jiang, and Yugui Yao (2011). *Low-energy effective Hamiltonian involving spin-orbit coupling in silicene and two-dimensional germanium and tin*, Phys. Rev. B 84, 195430.